Chin. Geogra. Sci. 2016 Vol. 26 No. 2 pp. 229–243
doi: 10.1007/s11769-016-0802-5

Springer Science Press
www.springerlink.com/content/1002-0063

Using Impervious Surfaces to Detect Urban Expansion in Beijing of China in 2000s

PENG Jian, LIU Yanxu, SHEN Hong, XIE Pan, HU Xiaoxu, WANG Yanglin

(*Laboratory for Earth Surface Processes*, *Ministry of Education*, *College of Urban and Environmental Sciences*, *Peking University*, *Beijing* 100871, *China*)

Abstract: The change of impervious surface area (ISA) can effectively reveal the gradual process of urbanization and act as a key index for monitoring urban expansion. Experiencing rapid growth of the built environment in the 2000s, urban expansion of Beijing has not been fully characterized through ISA. In this study, Landsat TM images of Beijing in 2001 and 2009 were obtained, and the eight-year urban expansion process in Beijing was analyzed using the ISA extracted by means of the vegetation-imperious surface-soil (V-I-S) model. From the spatial variation in ISA, the ring structure of urban expansion in Beijing was significant during the study period, with decreasing urban density from the city center to the periphery. In the ring road analysis, the most dramatic changes of ISA were found between the fifth ring and the sixth ring. This area has experienced the most new residential development, and is currently the main source of urban expansion. The typical profile lines revealed the directional characteristics of urban expansion. The east-west profile was the most urbanized axes in Beijing, while ISA change in the east-north profile was more significant than in the other five profiles. Moreover, the transition matrix of ISA levels revealed an increase in urban density in the low density built areas; the Moran′s I index showed a clear expansion of the central urban area, which spread contiguously; and the standard deviational ellipse indicated the northeast was the dominant direction of urban expansion. These findings can provide important spatial control guidelines in the next round of national economic and social development planning, overall urban and rural planning, and land use planning.

Keywords: impervious surface area (ISA); vegetation-imperious surface-soil (V-I-S) model; profile line analysis; urban expansion direction; Beijing, China

Citation: Peng Jian, Liu Yanxu, Shen Hong, Xie Pan, Hu Xiaoxu, Wang Yanglin, 2016. Using impervious surfaces to detect urban expansion in Beijing of China in 2000s. *Chinese Geographical Science*, 26(2): 229–243. doi: 10.1007/s11769-016-0802-5

1 Introduction

Since the period of reform and opening up in the 1980s, all aspects of China′s economy and society have undergone considerable development, with urbanization increasing at a dramatic rate. However, due to increased economic demand, the cities, and especially the large metropolitan areas, have experienced rapid expansion of the built environment, which has placed considerable stress on the natural environment (Liu *et al.*, 2012). By the end of 2010, China had a population of nearly 1.4×10^9. In spite of its vast territory, the amount of land suitable for human inhabitation and meeting basic conditions for social development is quite limited. The population distribution is uneven, as about 46% of the population lives in cities where the main land use type is impervious surface. Impervious surface has been an important characteristic of urbanization (Li *et al.*, 2013). At regional scale, the expansion of impervious surface damages the surrounding vegetation and profoundly influences the thermal environment and water ecosystem in the city (Liu *et al.*, 2010; Cai *et al.*, 2012). Thus,

Received date: 2015-05-08; accepted date: 2015-08-05
Foundation item: Under the auspices of Key Project of National Natural Science Foundation of China (No. 41130534)
Corresponding author: PENG Jian. E-mail: jianpeng@urban.pku.edu.cn

detecting landscape characteristics and associated changes in impervious surface area (ISA) has become an important objective in monitoring the dynamics of urbanization.

Land use/land cover change research based on discrete spatial data (i.e., remote sensing image pixels) has been the basic paradigm of research on the dynamics of urbanization. However, because each pixel can only represent one kind of land use type, discrete spatial images usually eliminate the characteristic of mixed land covers, thereby obscuring the gradual pace of ecological change in the process of urbanization (King *et al*., 2005; Peng *et al.*, 2006). Extracted by means of the vegetation-imperious surface-soil (V-I-S) model, ISA is a kind of continuous spatial data, which can be used to comprehensively measure changes in land use intensity and magnitude in cities. As an important link between landscape pattern changes and the ecological effects in the process of urbanization, ISA can quantitatively reveal urban landscape dynamics and change gradients. Thus, ISA is an effective indicator for measuring urbanization and its ecological effects because it can effectively couple landscape patterns with ecological processes.

ISA has already been widely used in estimating the spatial population distribution in residential areas, classifying land use and cover types, and recognizing urban environmental effects. In spatial population distribution studies, Wu and Murray (2005) built a correlation model between ISA and population data in Columbus using Cokriging model, with only –0.3% deviation. Lu *et al*. (2006) used ISA to estimate the population density in Marion (Indiana, USA), and found the linear regression model was applicable in cities where 25%–85% land were residential areas. In land use/land cover type classification studies, Rashed *et al.* (2001) divided the landscape of Cairo into such four parts as vegetation, imperious surface, soil, and shadow using the decision tree, with the accuracy of 0.88. Phinn *et al.* (2002) adopted V-I-S model to classify the Landsat TM image in the southwest of Queensland, and verified the accuracy of V-I-S model was higher than traditional methods based on over 900 reference sample points on four transects. To detect the environmental effects of urbanization, Zhou and Xu (2007) mapped the ISA in Fuzhou City and found that the increase of ISA had a negative impact on urban environment. It was also reported that ISA change would lead to the change of spatio-temporal water distribution, water quality and thus hydrological processes (Brabec, 2002; Jantz *et al.*, 2005; Liu *et al.*, 2010; 2013). Xie *et al.* (2009; 2013) adopted sub-pixel decomposition method to quantify the impact of ISA and other landscape pattern factors on urban thermal environment. All the case studies revealed that ISA is certainly an effective indicator in detecting urbanization and its ecological effects.

As the capital of China with urban area for nearly 100 km^2, Beijing is an inland city with hills and plain as the predominant landscape features. Since the founding of new China, Beijing has enjoyed unique political, information, technology, and talent advantages, which laid a strong foundation for social development and urban expansion. For decades, rapid growth of the built environment has promoted economic development, while conversely economic development has also accelerated human demanding for new construction land. Today, the inner city of Beijing is extending to the Sixth Ring Road. The scarcity of land is increasingly becoming the limiting factor in the further development of Beijing. Moreover, because buildings and infrastructure occupied so much land, there were few natural landscape patches with mixed patches for the majority (Qian *et al*., 2015). This situation leaded to a variety of ecological problems. Focusing on the ISA in Beijing, Li *et al.* (2011) discussed the influence of data spatial resolution on ISA extraction. Xiao *et al.* (2007) revealed the relationship between ISA and land surface temperature in the inner city of Beijing; Yuan *et al.* (2009) analyzed spatial distribution of ISA; and Li *et al.* (2013) determined the driving factors in impervious surface formation. Nevertheless, the characteristics of Beijing′s urban expansion as revealed by ISA were still sketchy. Further analysis would be required for the application of ISA to guide the next round of urban planning and spatial control. Thus, in this study, two periods of Landsat TM images were obtained in order to extract ISA, to analyze the temporal variation of spatial patterns, and to determine the recent spatial trends in urban expansion in Beijing. More specifically, the goals of this study were to measure ISA change from 2001 to 2009 in order to verify the ring structure of spatial variation, to identify directional characteristics of urban expansion based on typical profile line analysis, and to make clear spatial direction of urban expansion in Beijing using spatial statistical tools.

2 Materials and Methods

2.1 Study area

The total area of Beijing is 16 807.8 km^2, with about 160 km and 176 km for the distance from east to west, and from north to south, respectively. Mountainous area is about 10 417.5 km^2, accounting for 62% of the total area. The elevation of the mountainous area varies considerably, up to 2268 m. The plain area is about 6390.3 km^2, accounting for 38% of the total area. The elevation of the plain is less than 100 m, and the lowest elevation is only 6 m. The economic power of Beijing always ranks in the forefront of the country. Looking back at the economic development of Beijing from 2001 to 2009, GDP growth has always maintained a high level of more than 10% per year. Compared with the 2001 GDP of 2.818×10^{11} yuan (RMB), the 2009 GDP was four times larger. Compared with the 2001 per capita GDP of 2.53×10^4 yuan, the 2009 per capita GDP was three times larger. During 2001–2009, the total population has grew fast from1.39×10^7 to 1.76×10^7, which showed a high rate of population growth in the rapid urbanization of Beijing.

With the functional optimization and adjustment of Beijing, industrial activity spread to the suburbs, and it was gradually merged for the urbanization of the suburbs and suburbanization of the inner city (Zhang and Su, 2009). The implementation of the *Beijing Master Plan (2004–2020)* has had a significant impact on the functional organization of Beijing. The industrial and commercial functions in the inner city have been weakened, together with the strengthening of political and cultural functions. Therefore, the manufacturing industry has gradually shifted from the central city to the suburbs. A large number of industrial enterprises have also relocated from the city center and they have been replaced by other businesses. The tertiary industry, which includes the service sector, is gradually becoming the leading industry of the inner city. At the same time, the suburbs are gradually becoming the heart of the industrial distribution.

Beijing is made up of 16 administrative districts, with two in the inner city (Xicheng, and Dongcheng), four in the suburbs (Chaoyang, Haidian, Fengtai, and Shijingshan), and ten in the outer suburbs (Daxing, Tongzhou, Shunyi, Pinggu, Miyun, Huairou, Yanqing, Changping, Mentougou, and Fangshan). Since the *Beijing Outline of the Eleventh Five-Year Program for National Economic and Social Development* and the *Beijing Master Plan (2004–2020)* have been put into effect, Beijing has been divided into four functional zones (Fig. 1). These are the Core Function Zone (inner city), the Urban Function Extended Zone (Chaoyang, Fengtai, Haidian, and Shijingshan), the New Urban Development Zone (Tongzhou, Daxing, Shunyi, Changping, and Fangshan), and the Ecological Conservation Zone (Pinggu, Miyun, Yanqing, Mentougou, and Huairou).

2.2 Impervious surface area extraction

In order to solve the mixed pixel problem, imperious surface detection on a sub-pixel level has been developed in recent years. The spectral mixing analysis method has been widely used (Ichoku and Karnieli, 1996; Rashed *et al*., 2001). Based on the decomposition method, spectral mixing analysis can be divided into linear spectral mixture models (LSMM) and nonlinear models (Ichoku and Karnieli, 1996). Although the nonlinear models can better reduce the residual error and improve the accuracy of decomposition, they are more complex and hard to estimate accurately. LSMM has clear physical sense and is generally accepted as easy to handle, so it has become the most widely used model (Small, 2001; Small, 2002; Wu and Murray, 2003; Wu, 2004; Lu and Weng, 2006; Kuang *et al.*, 2011; Liu *et al.*, 2011; Wang *et al.*, 2011). In LSMM, the composition selection was the key process, and V-I-S model provides the theoretical foundation for this composition selection process (Ridd *et al*., 1995). The basic formula of LSMM is:

$$R_j = \sum_{i=1}^{n} f_i R_{ij} + e_j \tag{1}$$

$$f_i \geq 0 \,;\, \sum_{i=1}^{n} f_i = 1 \tag{2}$$

where R_j represents the pixel reflectance in j spectrum; n is the total number of endmember; f_i is the fraction of endmember i; R_{ij} represents pixel reflectance in j spectrum for endmember i; and e_j is error term of j spectrum.

In this study, four Landsat TM images were downloaded from Geospatial Data Cloud (http://www.gscloud.cn/), with the date of 2001/08/31 and 2009/09/22. Then the V-I-S model was adopted to extract ISA. The V-I-S model considers urban surface as composed of vegetation,

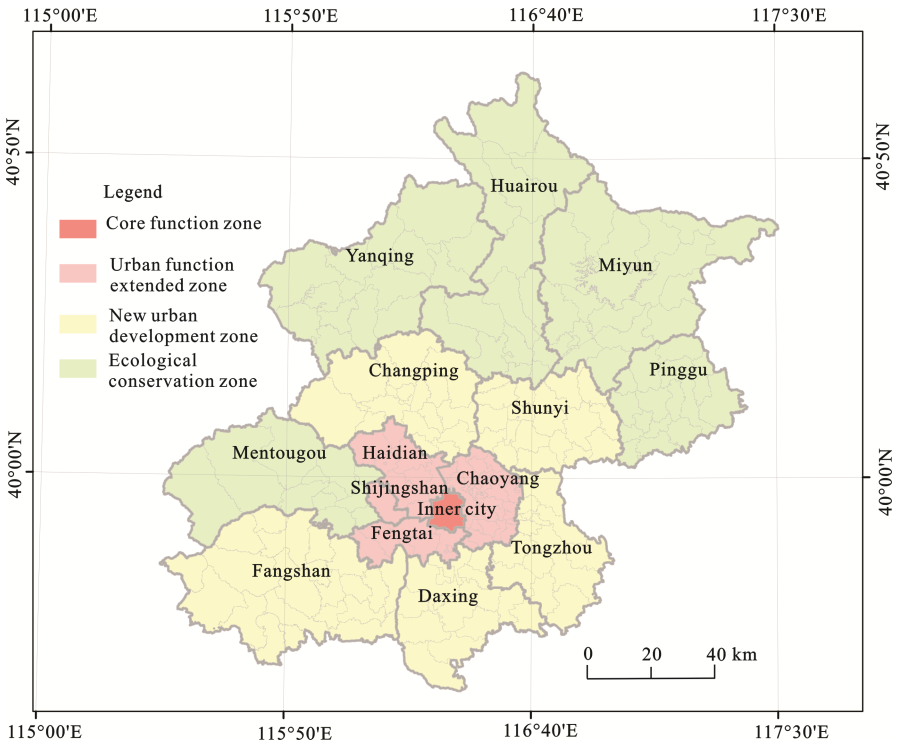

Fig. 1 Four functional zones of study area

impervious surface, and soil, with the three components in a mutually exclusive relationship on the remote sensing image. Associating features of urban landscape with the spectral character of the components has become one of the main methods in urban remote sensing. The Minimum Noise Fraction (MNF) and Pixel Purity Index (PPI) were adopted from LSMM in ENVI 5.0. MNF is a widely used spectrum transformation method that can effectively eliminate the high correlation between different bands of the original image and improve the quality of endmember selection (Emma *et al*., 2003; Zhang *et al*., 2003). After MNF transformation, the image information is highly concentrated in the front three bands. In Beijing inner city, the percent of image information in the front three bands was 97.52% in 2001 and 97.68% in 2009, and in the first band, the percentages were 90.11% and 91.50%. Therefore, the front three bands can be used as the basic dimensions for endmember selection.

Endmember selection can directly influence the model accuracy, and usually 3–4 endmembers are appropriate (Small, 2004). Because the high albedo surfaces of concrete and sand have similar reflectance vectors with soil endmember, we composed them as substrate endmember and determined three endmembers, namely the dark surface endmember, the vegetation endmember, and substrate endmember. Then we supposed the substrate endmember was all in cities and towns. PPI was adopted to define the purity of pixels (Yue, 2009). In this study, the iteration upper limit was set as 15 000, the threshold was 2.5, and the iteration of PPI more than 20 was adopted.

Considering that bodies of water and shadow are often misclassified in extracting ISA, methods of eliminating water and vegetation shade by mask were needed to correct the results of the initial analysis. In this study, the water mask was extracted by New Water Index (NWI), which mixed band 7 in TM (Ding, 2009). The vegetation shade was extracted by Normalized Difference Umbra Index (NDUI), which mixed the saturation and lightness (Zhou *et al.*, 2011). It was found that NDVI > 0.1 and NDUI > 0.4 can effectively eliminate the low albedo components in the shadow.

To detect the validity and accuracy of the ISA in this study, mean residual and root mean square error (RMSE) were adopted to analyze the model error:

$$RMSE = \sqrt{(\sum_{i=1}^{n} \varepsilon_{in}^2)/m} \tag{3}$$

where *RMSE* is the root mean square error which illus-

trated the distance of residual deviates from the average value; ε_{in} is the residual of pixel i in band n; and m is the number of pixel.

3 Results

3.1 Impervious surface area change in districts

In Beijing, the average ISA across districts increased from 24.44% in 2001 to 29.28% in 2009 (Fig. 2). The spatial pattern of ISA appeared as a ring structure with decreasing density from inner city to outer suburbs. In terms of different land use types, the higher value of ISA (64%–100%) corresponded to built-up areas, with a mean value of 86%. The lower value of ISA corresponded to the cultivated land, forest land, and grassland. The lowest values (0–18%) were found in forest land, with a mean value of 13%. From 2001 to 2009, the ISA increased for all land use types. The ISA in green areas increased the most at 5.24% (from 38.15% to 43.38%).

At the district scale, the ISA in different functional zones varied widely but had strong consistency in the same zone (Table 1). Due to the highly dense construction, the ISA in the Core Function Zone was obviously higher than the surrounding area. In 2001 and 2009, it reached 82.04% and 81.30% respectively. Nevertheless, the ISA growth showed a negative trend of –0.74% due to a shift in the core city function. Over the eight-year period, some built-up areas for traditional industry and logistics were abandoned, reducing the total built-up area by 4.51 km^2. At the same time, the ancient capital's ecological outlook was improved as the green space in the inner city expanded by 3.27 km^2. As the high tech industry base and education center, the Urban Function Extended Zone had relatively high ISA overall. All the ISA in the four districts of this zone were higher than 43% in 2001 and higher than 52% in 2009. In Chaoyang in particular, the ISA reached 54.06% in 2001 and 66.87% in 2009, with an increase of 12.81%. The ISA in Shijingshan grew the slowest because population growth was relatively low in this district. In the New Urban Development Zone, the ISA ranged from 24.02% to 41.63%. The highest ISA was in Tongzhou, which reached 37.37% in 2001 and 41.63% in 2009. In terms of growth, Tongzhou and Changping were the most active, with an increase of more than 4.2% in each district, and Shunyi grew the slowest. The ISA change in this zone was the effect of urban expansion and a resulting decrease in vegetation. As the ecological boundary and environmentally friendly industrial base of Beijing, the Ecological Conservation Zone had low ISA that ranged from 13.81% to 24.75%. In Pinggu, the ISA reached 18.81% in 2001 and 24.75% in 2009, which is the highest among districts in this zone. Mentougou increased the slowest at only 1.24%. Apart from urban expansion, forest decline was also a driving factor in increasing ISA.

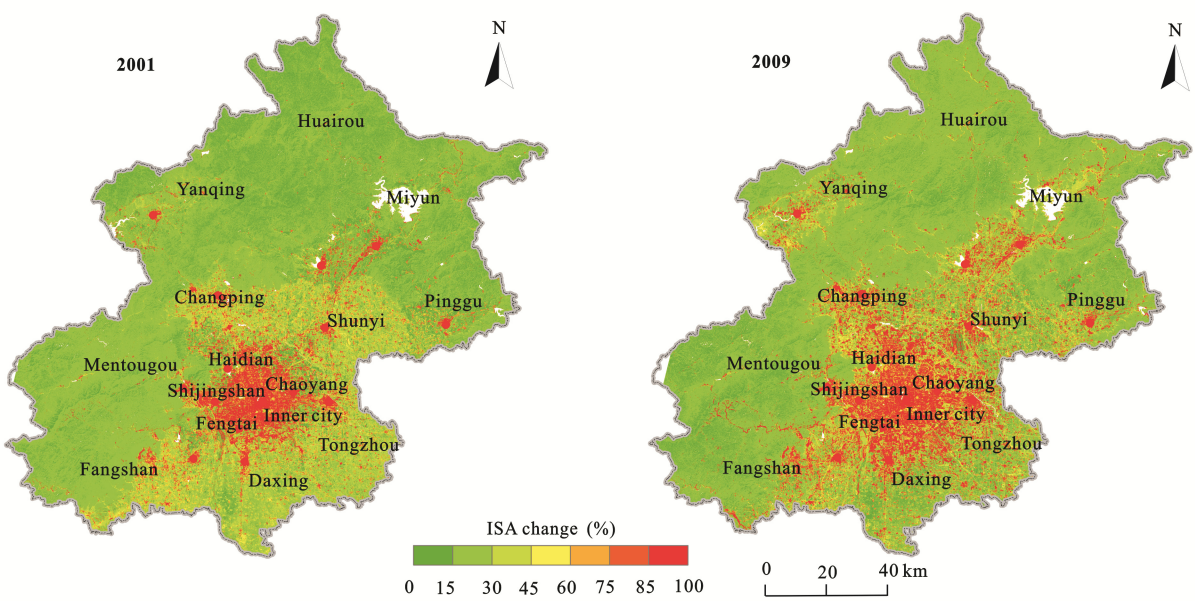

Fig. 2 Impervious surface area (ISA) change in Beijing during 2001–2009

3.2 Impervious surface area change in ring roads

The ring road is a key framework of the urban transportation network in Beijing, and five ring roads have been constructed to keep pace with the rapid urban expansion (Fig. 3). On the one hand, the ring roads have helped to balance space requirements, mitigating the single center polarization phenomenon. One the other hand, the close proximity of the ring roads has further concentrated the urban built environment, which has gradually extended from the inner city outward. Thus, characterizing the spatial pattern of ISA in the areas between the ring roads is helpful in describing the urban expansion in Beijing.

Analysis of ISA in the areas between the ring roads showed a decrease in the density of the built environment but an increasing rate of new construction from inner city to outer suburbs (Table 2). The ISA was higher than 82% inside the second ring, higher than 79% in the second to third ring, and higher than 76% in the third to fourth ring. In terms of ISA change, the dynamic was relatively steady inside the fourth ring, which revealed that highly urbanized space had been stable in the scale of construction and focused on functional optimization rather than urban expansion. The negative ISA growth inside the third ring reflected the relocation of traditional industry and the promotion of green areas. The most dramatic ISA change happened in the outer rings, with a growth of 7.34% between the fourth and fifth ring and 11.87% between the fifth and sixth ring. This region was the interface between the Urban Function Extended Zone and New Urban Development Zone (Fig. 1) with many large residential clusters, where the most significant urban expansion had taken place. The ISA was relatively low outside the sixth ring, but the growth was 4.20%. The active growth was due to the new urban development in the suburbs.

Table 1 Change in impervious surface area from 2001 to 2009

Functional zone	Name	Mean impervious surface area in 2001 (%)	Standard deviation of impervious surface area in 2001	Mean impervious surface area in 2009 (%)	Standard deviation of impervious surface area in 2009	Growth of mean impervious surface area (%)
Core function zone	Inner city	82.04	0.1735	81.30	0.1623	–0.74
Urban function extended zone	Chaoyang	54.06	0.3403	66.87	0.2738	12.81
	Fengtai	53.78	0.3326	62.26	0.2855	8.48
	Haidian	43.89	0.3340	52.05	0.2879	8.16
	Shijingshan	50.04	0.3388	55.55	0.3125	5.51
New urban development zone	Tongzhou	37.37	0.2062	41.63	0.2869	4.26
	Daxing	35.11	0.1958	38.01	0.2926	2.90
	Shunyi	36.65	0.2053	38.55	0.2746	1.90
	Changping	27.20	0.2139	31.70	0.2659	4.50
	Fangshan	24.02	0.1887	26.51	0.2404	2.49
Ecological conservation zone	Pinggu	18.81	0.1725	24.75	0.2039	5.94
	Miyun	15.70	0.1531	22.97	0.1937	7.27
	Yanqing	15.16	0.1254	21.65	0.1631	6.49
	Huairou	13.81	0.1332	20.19	0.1568	6.38
	Mentougou	15.32	0.1163	16.56	0.1535	1.24

Table 2 Variation of impervious surface area based on ring road

Ring	Mean impervious surface area in 2001 (%)	Standard deviation of impervious surface area in 2001	Mean impervious surface area in 2009 (%)	Standard deviation of impervious surface area in 2009	Growth of mean impervious surface area (%)
Inside second ring	82.97	0.1504	82.13	0.1454	–0.84
Second to third ring	79.78	0.2021	79.43	0.1804	–0.35
Third to fourth ring	76.14	0.2577	76.99	0.2147	0.85
Fourth to fifth ring	61.19	0.3110	68.53	0.2653	7.34
Fifth to sixth ring	41.80	0.2792	53.67	0.3063	11.87
Outside sixth ring	20.22	0.1721	24.42	0.2091	4.20

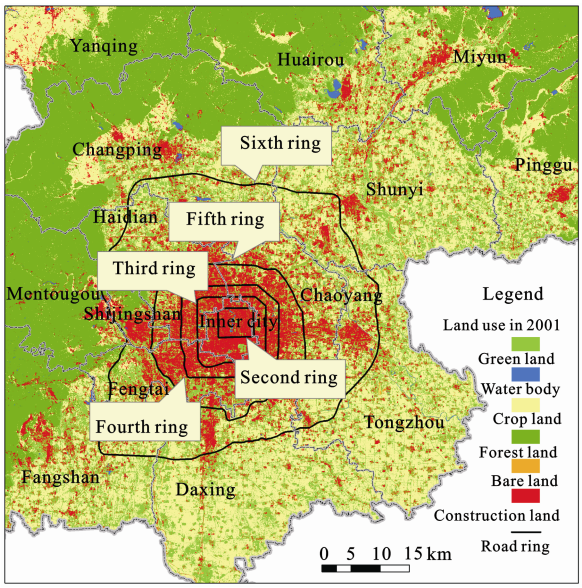

Fig. 3 Ring roads of Beijing (second to sixth)

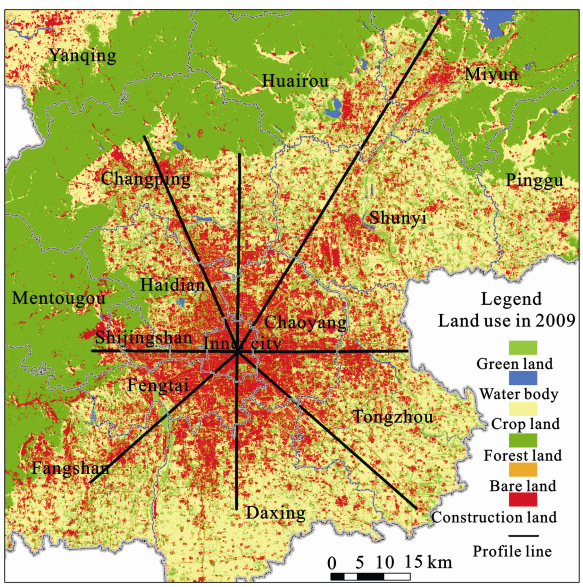

Fig. 4 Typical profile lines in Beijing

3.3 Impervious surface area change in profile lines

In the *Beijing Master Plan (2004–2020)*, the city could be portrayed as two axes, two belts, and several centers. In order to detect the pixel differences in ISA, six typical profile lines were adopted to cover the axes and belts, as well as to connect the centers (Fig. 4). The width of the profile line was 120m.The east-west profile was the extension line of Chang′an Street. Its western starting point was Yongding Town in Mentougou, and the east endpoint was the new urban development area in Tongzhou. The south-north profile was the central axis of Beijing across the Imperial Palace. The south starting point was Daxing and the north endpoint was Xiaotangshan Town in Changping. The east-north profile and east-south profile were in the eastern development belt. The west-north profile and west-south profile were in the western development belt. The ends of the four profiles were Miyun, Yongdian Town in Tongzhou, Nankou Town in Changping, and the new urban development area in Fangshan, respectively.

As it ran through the main political and economic function zone of Beijing, the east-west profile was the earliest and most highly developed city axis. Except for the suburb of Yongding Town in Mentougou, the Shijingshan Forest Park, and the Chaoyang Park, the ISA in most of the pixels was higher than 65%. For the fluctuation of the east-west profile, the degree of change on the eastern side was far higher than on the western side, and the middle section from Haidian to Chaoyang was stable (Fig. 5). The Dingfuzhuang residential cluster in Chaoyang varied the most at nearly 15% on average. The south-north profile was a major corridor between the ancient capital and modern city. The profile showed a typical parabolic shape which fluctuated more sharply than the east-west profile. In the south, the construction land increased fast due to the rapid development of Nanyuan residential cluster and the new urban development area in Daxing, with an average growth of 25%. In the north, the construction of the Olympic Sports Center and the development of Qinghe and Beiyuan residential cluster raised the average growth to 12%.

The trend lines in the east-north profile and east-south profile were roughly the same, where the ISA gradually reduced from inner city to Miyun and Tongzhou, respectively (Fig. 6). In the east-north profile, the ISA in most pixels grew significantly, except in the inner city. In the Jiuxianqiao residential cluster in Chaoyang, the Capital International Airport group in Shunyi, and the new urban development area in Huairou and Miyun, the growth was 13%–30%. In the east-south profile, the ISA in the new urban development area in Yizhuang and Yongle grew 8%–25%. The axis from Yizhuang to Yongle constituted a major corridor connecting Beijing and Tianjin City, which became a core section of ISA growth.

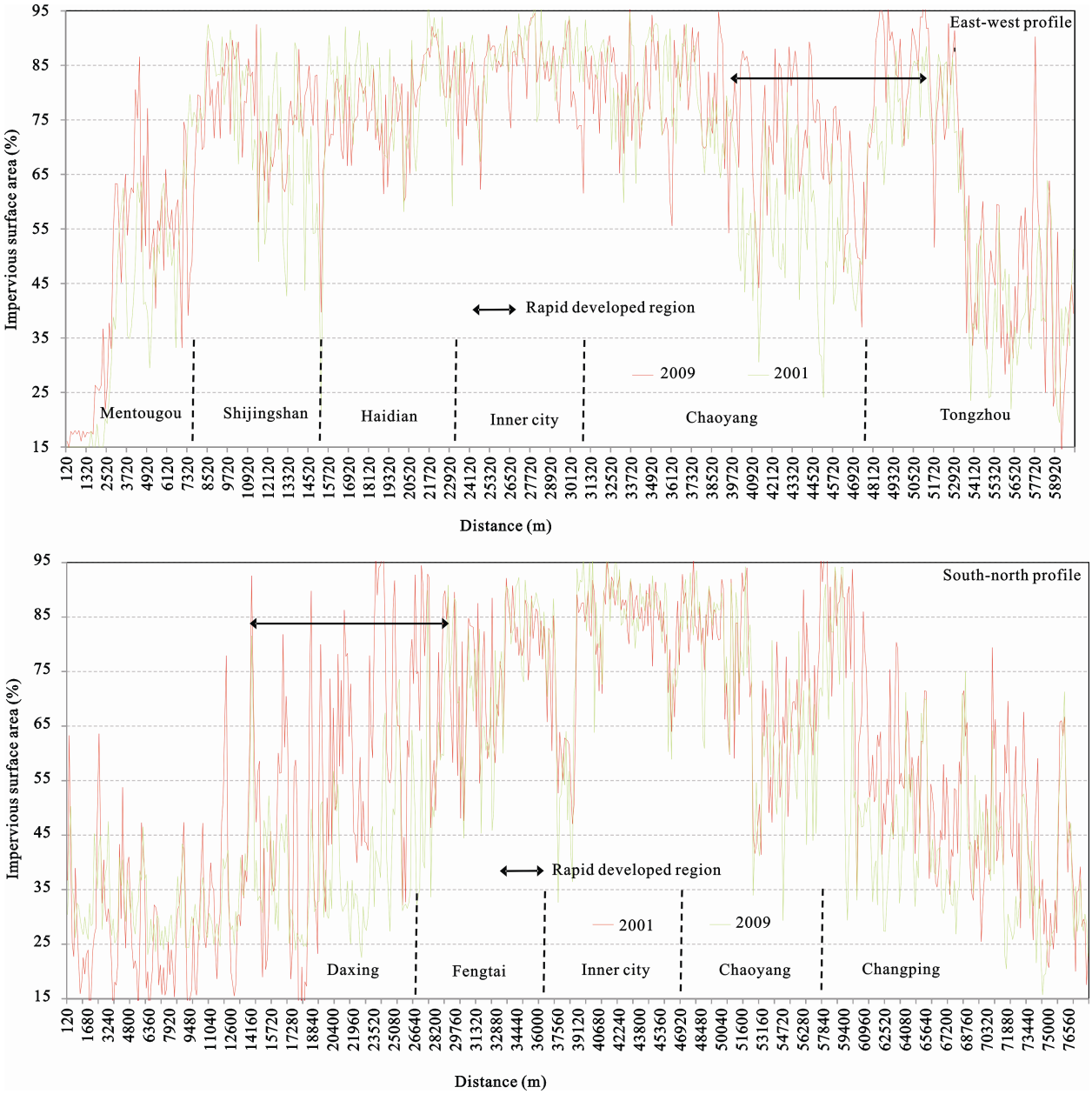

Fig. 5 Variation of impervious surface area in east-west profile and south-north profile

The west-north profile revealed a trend from a decline to an increase (Fig. 7). From the inner city to the Beiyuan residential cluster, the ISA was greater than 60% on average. Moving further north, the ISA dropped for the mixed land use type in the suburban belt between Haidian and Changping. However, the ISA at the north end of the profile in Changping was higher than most of the ISA in Haidian. The fastest growth was in the northwest of Haidian with a range of 9%–16%. The ISA in the west-south profile experienced a clear increase between Fengtai and Liangxiang Town in Fangshan, with an average growth of 10%–30%. Fengtai is located between the fourth and fifth ring road and was one of the key sections for inner city expansion. Liangxiang Town was the core part of the new urban development area in Fangshan and the infrastructure for industry increased considerably from 2001 to 2009.

4 Discussion

4.1 Quantifying urban expansion

In order to recognize the main characteristics of urban

expansion, spatial statistical analysis was needed to examine the spatial and temporal patterns of ISA change. Seven levels of ISA were reclassified with 15%, 30%, 45%, 60%, 75%, and 85% as the intervals to form a transition matrix (Table 3). Compared with the land use map, it had been found that the area of 45% level was most close to the area of construction land. Thus, ISA > 45% were set as urban built-up area. In concrete terms, Moran′s I index was adopted to analyze the spatial agglomeration of the urban built-up environment. Then Median Center and Standard Deviational Ellipse were utilized to determine the spatial trends in built-up area. These algorithms were implemented with the Spatial Statistics Tools in ArcGIS 10.2. As the transition matrix showed, 29.40% of the pixel levels increased and 18.25% of them decreased. The other 52.35% pixel levels remained unchanged. Overall, there was a visible upward trend in ISA level. A large number of pixels at the level of medium to high changed to very high level, which showed that many of the lower density built-up areas continued to increase.

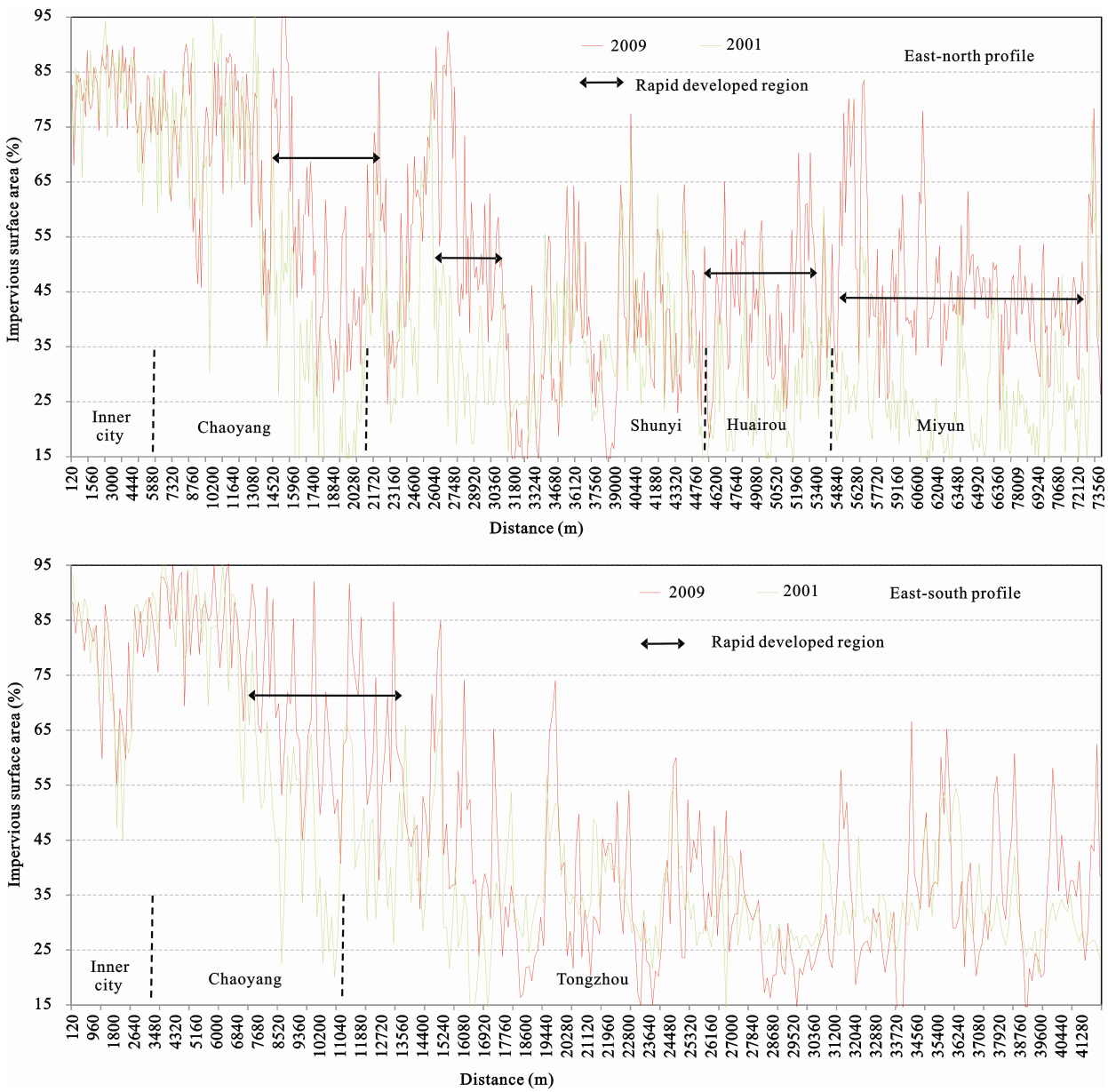

Fig. 6 Variation of impervious surface area in east-north profile and east-south profile

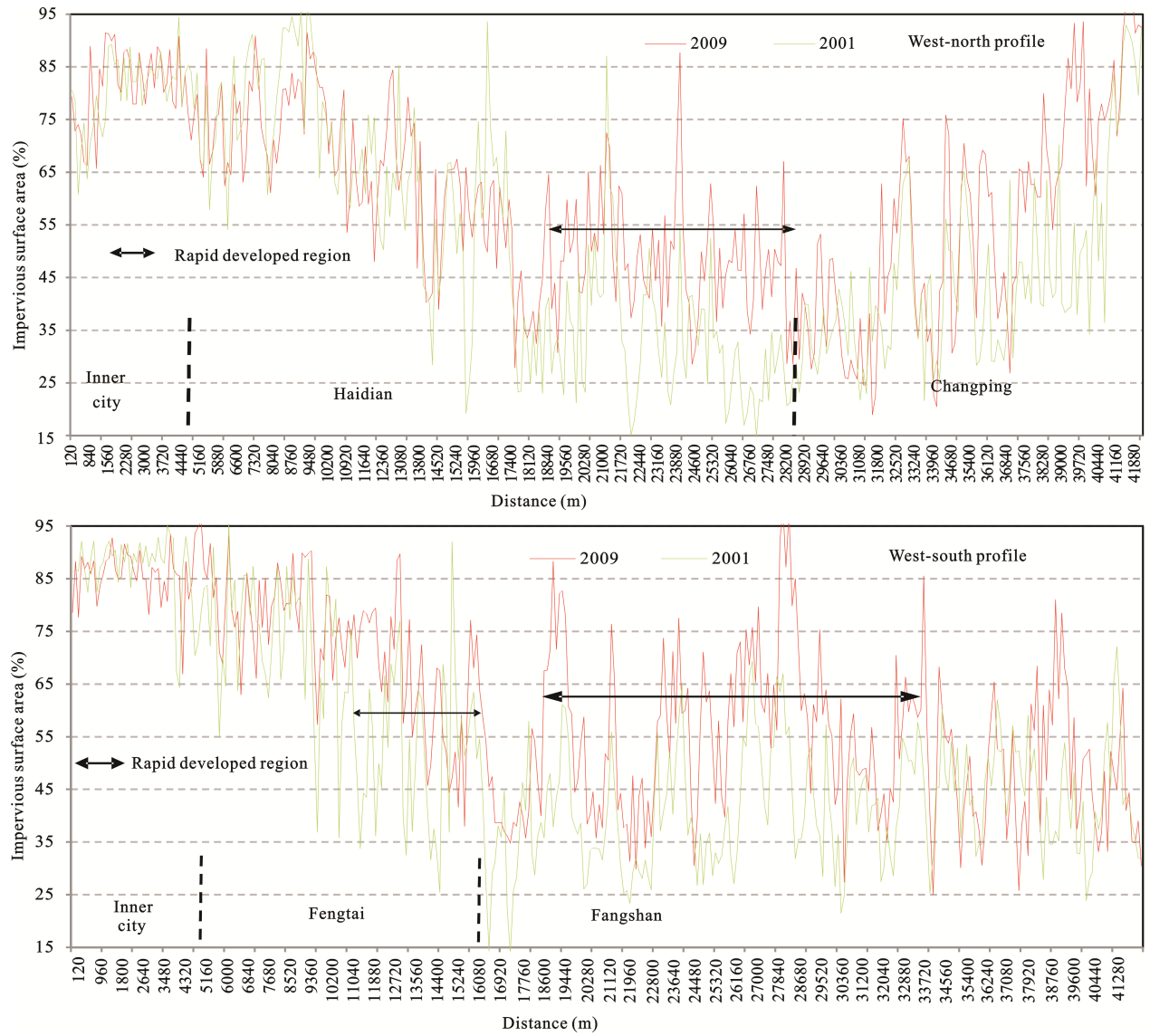

Fig. 7 Variation of impervious surface area in west-north profile and west-south profile

Table 3 Impervious surface area level transition matrix (km^2)

2009 \ 2001	Very low	Low	Relatively low	Medium	Relatively high	High	Very high
Very low	877.75	1240.75	208.16	16.63	4.64	14.37	15.19
Low	2075.37	6338.62	708.67	64.85	18.57	58.75	43.29
Relatively low	202.30	663.37	568.12	120.38	23.06	83.08	63.53
Medium	33.67	124.37	153.67	83.87	16.65	44.02	34.45
Relatively high	15.07	65.30	48.06	21.97	12.74	26.41	20.35
High	48.83	184.70	159.01	51.33	21.69	133.39	120.38
Very high	82.13	259.09	203.96	71.48	30.41	230.67	437.19

Due to spatial interaction and diffusion of geographical processes, the geographical data may not be independent, but interrelated. Moran′s I, as a classic spatial autocorrelation algorithm, can effectively identify the high-low agglomeration relationship on space (Xie *et al*., 2013). At the town scale in 2001 and 2009 (Fig. 8), the low-low agglomeration samples were both 44, but the amount decreased in the north and increased in the

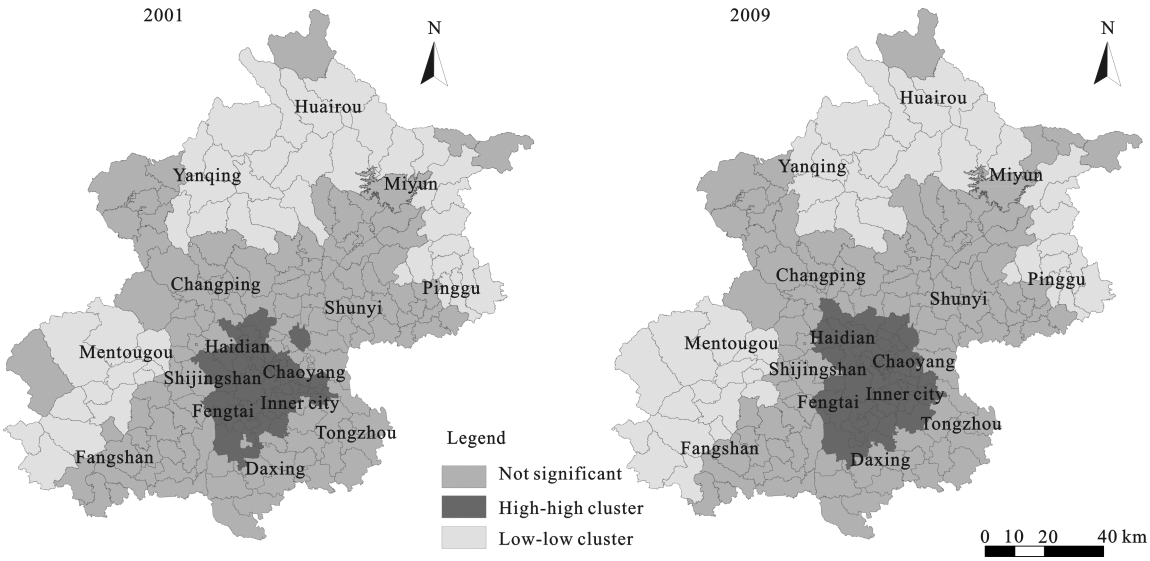

Fig. 8 Spatial autocorrelation change of ISA at town level in Beijing during 2001–2009

west. The high-high agglomeration samples were 47 in 2001 but increased to 59 in 2009, forming a more concentrated spatial pattern in the center of Beijing. This trend indicated that the main urban area expanded considerably in a contiguous sprawl pattern. However, the agglomeration only expresses relative change, not the absolute value. As the ISA levels mostly increased in 2009, the new low-low agglomeration might not mean a decrease in ISA in 2009, but an increase of the ISA in surrounding samples that flattened the difference. Likewise, in the background of an overall increase in ISA, the new high-high agglomeration should not be ascribed to a decrease in the inner city, but it could more likely be due to a rapid increase of ISA in the suburbs.

In order to determine the direction of urban expansion, the median center and standard deviational ellipse of the urban built-up area were calculated (Fig. 9). The Median Center tool was a measure of central tendency, which identified the location that minimized travel from it to all other features in the dataset, and could be used as a feature distribution measurement. The Standard Deviational Ellipse tool created a new feature class containing an elliptical polygon centered on the mean center for all features that could be used to detect the feature dispersion and directional trends. When the features were densest in the center and became less dense toward the periphery, one standard deviation would encompass approximately 68% of all input features. The result showed that the median center in 2009 was 3 km northeast of the median center in 2001. This indicated that ISA increased more rapidly in the northeast than in the southwest. In the standard deviational ellipses, the major axis pointed toward the northeast, and the most significant expansion from 2001 to 2009 was along this axis. This indicated that the northeast was the main direction of urban growth, driven by new construction in the east, north, and northeast. In this area, Chaoyang became the newly developed financial district, and Tongzhou and Shunyi became new centers of urban development. These districts enjoyed the opportunity policy and had substantial resources at their disposal for modernization. Construction projects such as the capital airport, Olympic venues, and the high-speed road built in Shunyi accounted for part of the increase in ISA in this direction. In contrast, the southwest elliptic boundary barely moved from 2001 to 2009, suggesting that urban expansion in the southwest was relatively negligible.

4.2 Uncertainty and future research directions

As the accuracy evaluation shown (Table 4), except for the suburb of 2001, which had a mean residual of 0.039, the other mean residuals were all below 0.03. The overall accuracy of the compositions from V-I-S model was high. Especially in the suburb of 2009, the mean residual was 0.021 and RMSE was 0.012. The other RMSEs were between 0.014 and 0.026, which is lower than the 0.32–1.40 of RMSE for Beijing′s ISA in another published study (Yuan *et al*., 2009). Moreover, it was found that the high residuals were usually distributed in the built-up areas. Because urban landscape had strong

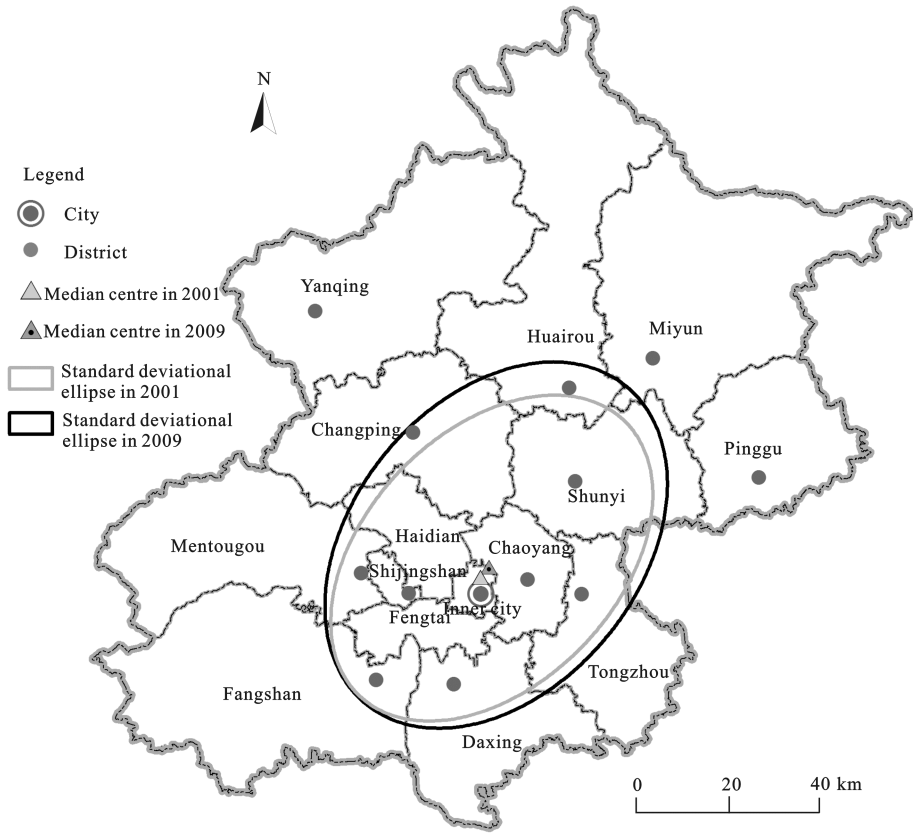

Fig. 9 Median center and standard deviational ellipse of urban built-up area from 2001 to 2009

Table 4 Mean residual and root mean square error (RMSE) from V-I-S model

Image	Pixel number	Mean residual	Root mean square error
Inner city of 2001	2 493 789	0.025	0.021
Inner city of 2009	2 493 789	0.024	0.018
Suburb of 2001	15 754 832	0.039	0.026
Suburb of 2009	15 754 832	0.021	0.012
Outer suburbs of 2001	19 199 320	0.027	0.017
Outer suburbs of 2009	19 199 320	0.028	0.015

spatial heterogeneity and complex surface cover, it was hard to extract pixels of ideal purity. In spite of the built-up areas, 99% of the residuals were less than 0.05 with a spatially random distribution. Finally, the overall RMSE was 0.029, which also indicated to a credible result.

In the process of endmember selection in this study, pure pixels of vegetation were most common and easiest to extract; pure pixels of soil were less common but easy to distinguish; low albedo surface was easily mixed with river; and high albedo surface was uncommon. The reason there were few high albedo surface pixels was that tall buildings with high albedo materials were discontinuous and occupied only a small area. As a result, these pixels could not be regarded as pure. Moreover, as the high albedo pixel was similar in spectrum characteristics to clouds, the choice was made more cautiously. The conservative endmember selection might lead to deviations from the typical spectral curve. In future studies, it is necessary to update the data source and algorithm for a higher accuracy of ISA extraction in the urban built environment (Li *et al*., 2011; Michishita *et al*., 2012).

Recognizing the mechanisms of urban expansion process from different driving forces and quantifying the negative effects on urban environment from impervious surface increase are two important directions in analyzing urban problems with the application of ISA. On the one hand, based on the quantitative measurements of natural indexes such as roads, rivers, and elevation, there is a key direction for a next-step study for how to characterize the relationship among various human activity factors such as landscape planning, economic development, and residents′ demands. On the other hand,

although some progresses have been achieved in investigating the relationship between impervious surface and urban heat environment (Li *et al*., 2012; Qiao *et al*., 2013; Quan *et al*., 2014), the correlations with other environmental indicators still need to be further studied. Paying attention to the relationship between the environmental indicators of water quality, air quality, and vegetation growth, and the impervious surface is an effective way to understand the evolving ecological impact of urban development. Thus, apart from urban landscape patterns formation, urban expansion processes, and driving forces of impervious surface change, there exists a key field to clarify the ecological effects due to urbanization with dramatic changes in landscape patterns.

5 Conclusions

ISA change can reveal the gradual spatial patterns associated with urbanization, which is a key indicator for evaluating urban expansion. In this study, V-I-S model was adopted to extract the ISA in Beijing from 2001 to 2009. Based on the temporal and spatial dynamic analysis of ISA, it was determined that the urban expansion process in Beijing had the following characteristics:

(1) The urban expansion in Beijing exhibited a recognizable ring structure, with decreasing urban density from the center to the periphery. In the Core Function Zone, with the adjustment and optimization of industrial structure, the ISA level experienced a slight decrease. In the Urban Function Extended Zone, the ISA level in Haidian, Chaoyang, and Fengtai increased significantly. In the New Urban Development Zone, the ISA in Tongzhou and Daxing was high and increased considerably. In the Ecological Conservation Zone, the ISA level was relatively low but the growth was also significant.

(2) The temporal and spatial dynamics were also distinctive in the ring road analysis. The ISA levels inside the fourth ring were generally stable, while the most dramatic growth occurred between the fourth ring and the sixth ring, especially in the fifth to sixth ring area. This region was the interface between Urban Function Extended Zone and New Urban Development Zone with many large residential clusters. The ISA level transition matrix also showed many of the lower density built-up areas continued to increase in density. As many of the lower density built-up areas could be found between the fourth ring and the sixth ring in 2001, the result indicated that this ring area was currently the main source of urban expansion.

(3) The typical profile analysis on urban spatial structure at the pixel level showed the east-west profile was the most urbanized axis. As the extension of the central axis of Beijing, the south-north profile had high ISA levels, with a more dramatic rate of growth in the south than in the north. The east-north profile, east-south profile, west-north profile, and west-south profile were the principle connection axes for the new urban development area, where the city expanded considerably. ISA growth in the east-north profile was most significant, which could be confirmed by the median center and standard deviational ellipse of the built-up area. Thus, it was found that from 2001 to 2009, the main direction of urban expansion in Beijing was northeast.

References

Brabec E, 2002. Impervious surfaces and water quality: a review of current literature and its implications for watershed planning. *Journal of Planning Literature*, 16: 499–514. doi: 10.1177/088541202400903563

Cai Yuanbin, Zhang Hao, Pan Weibin *et al*., 2012. Urban expansion and its influencing factors in natural wetland distribution area in Fuzhou City, China. *Chinese Geographical Science*, 22(5): 568–577. doi: 10.1007/s11769-012-0564-7

Ding Feng, 2009. A new method for fast information extraction of water bodies using remotely sensed data. *Remote Sensing Technology and Application*, 24(2): 167–171. (in Chinese)

Emma U, Susan U, Deanne D, 2003. Mapping nonnative plants using hyperspectral imagery. *Remote Sensing of Environment*, 86: 150–161. doi: 10.1016/S0034-4257(03)00096-8

Ichoku C, Karnieli A, 1996. A review of mixture modeling techniques for sub-pixel land cover estimation. *Remote Sensing Reviews*, 13: 161–186. doi: 10.1080/02757259609532303

Jantz P, Goetz S, Jantz C, 2005. Urbanization and the loss of resource lands in the Chesapeake Bay Watershed. *Environmental Management*, 36: 808–825. doi: 10.1007/s00267-004-0315-3

King R S, Baker M E, Whigham D F *et al*., 2005. Spatial considerations for linking watershed land cover to ecological indicators in streams. *Ecological Applications*, 15(1): 137–153. doi: 10.1890/04-0481

Kuang Wenhui, Liu Jiyuan, Lu Dengsheng *et al*., 2011. Pattern of impervious surface change and its effect on water environment in the Beijing-Tianjin-Tangshan Metropolitan Area. *Acta Geographica Sinica*, 66(11): 1486–1496. (in Chinese)

Li W F, Ouyang Z Y, Zhou W Q *et al*., 2011. Effects of spatial resolution of remotely sensed data on estimating urban imper-

vious surfaces. *Journal of Environmental Sciences*, 23(8): 1375–1383. doi: 10.1016/S1001-0742(10)60541-4

Li X M, Zhou W Q, Ouyang Z Y *et al*., 2012. Spatial pattern of greenspace affects land surface temperature: evidence from the heavily urbanized Beijing metropolitan area, China. *Landscape Ecology*, 27(6): 887–898. doi: 10.1007/s10980-012-9731-6

Li X M, Zhou W Q, Ouyang Z Y, 2013. Forty years of urban expansion in Beijing: what is the relative importance of physical, socioeconomic, and neighborhood factors? *Applied Geography*, 38: 1–10. doi: 10.1016/j.apgeog.2012.11.004

Liu Jiyuan, Zhang Qian, Hu Yunfeng, 2012. Regional differences of China′s urban expansion from late 20th to early 21st century based on remote sensing information. *Chinese Geographical Science*, 22(1): 1–14. doi: 10.1007/s11769-012-0510-8

Liu Z H, Wang Y L Li Z G *et al*., 2013. Impervious surface impact on water quality in the process of rapid urbanization in Shenzhen, China. *Environmental Earth Sciences*, 68(8): 2365–2373. doi: 10.1007/s12665-012-1918-2

Liu Zhenhuan, Wang Yanglin, Peng Jian *et al*., 2011. Using ISA to analyze the spatial pattern of urban land cover change: a case study in Shenzhen. *Acta Geographica Sinica*, 66(7): 961–971. (in Chinese)

Liu Zhenhuan, Li You, Peng Jian, 2010. Remote sensing of impervious surface and its applications: a review. *Progress in Geography*, 29(9): 1143–1152. (in Chinese)

Lu D S, Weng Q H, 2006. Use of impervious surface in urban land use classification. *Remote Sensing of Environment*, 102: 146–160. doi: 10.1016/j.rse.2006.02.010

Lu D S, Weng Q H, Li G Y, 2006. Residential population estimation using remote sensing derived impervious surface. *International Journal of Remote Sensing*, 27: 3553–3570. doi: 10.1080/01431160600617202

Michishita R, Jiang Z, Xu B, 2012. Monitoring two decades of urbanization in the Poyang Lake area, China through spectral unmixing. *Remote Sensing of Environment*, 117: 3–18. doi: 10.1016/j.rse.2011.06.021

Peng Jian, WangYanglin, Zhang Yuan *et al*., 2006. Research on the influence of land use classification on landscape metrics. *Acta Geographica Sinica*, 61(2): 157–168. (in Chinese)

Phinn S, Stanford M, Murray A T, 2002. Monitoring the composition of urban environments based on the vegetation impervious surface-soil model by sub-pixel analysis techniques. *International Journal of Remote Sensing*, 23: 4131–4153. doi: 10.1080/01431160110114998

Qian Yuguo, Zhou Weiqi, Yu Wenjuan *et al*., 2015. Quantifying spatiotemporal pattern of urban greenspace: new insights from high resolution data. *Landscape Ecology*, 30(7): 1165–1173. doi: 10.1007/s10980-015-0195-3

Qiao Z, Tian G J, Xiao L, 2013. Diurnal and seasonal impacts of urbanization on the urban thermal environment: a case study of Beijing using MODIS data. *ISPRS Journal of Photogrammetry and Remote Sensing*, 85: 93–101. doi: 10.1016/j.isprsjprs.2013.08.010

Quan J L, Chen Y H, Zhan W F *et al*., 2014. Multi-temporal trajectory of the urban heat island centroid in Beijing, China based on a Gaussian volume model. *Remote Sensing of Environment*, 149: 33–46. doi: 10.1016/j.rse.2014.03.037

Rashed T, Weeks J R, Gadalla M S *et al*., 2001. Revealing the anatomy of cities through spectral mixture analysis of multispectral satellite imagery: a case study of the Greater Cairo Region, Egypt. *Geocarto International*, 16(4): 7–18. doi: 10.1080/10106040108542210

Ridd M K, 1995. Exploring a V-I-S (vegetation-imperious surface-soil) model for urban ecosystem analysis through remote sensing: comparative anatomy for cities. *International Journal of Remote Sensing*, 16: 2165–2185. doi: 10.1080/01431169508954549

Small C, 2001. Estimation of urban vegetation abundance by spectral mixture analysis. *International Journal of Remote Sensing*, 22: 1305–1334. doi: 10.1080/01431160151144369

Small C, 2002. Multi temporal analysis of urban reflectance. *Remote Sensing of Environment*, 81: 427–442. doi: 10.1016/S0034-4257(02)00019-6

Small C, 2004. The Landsat ETM+ spectral mixing space. *Remote Sensing of Environment*, 93: 1–17. doi: 10.1016/j.rse.2004.06.007

Wang Hao, Wu Bingfang, Li Xiaosong *et al*., 2011. Extraction of impervious surface in Hai Basin using remote sensing. *Journal of Remote Sensing*, 15(2): 394–400. (in Chinese)

Wu C S, 2004. Normalized spectral mixture analysis for monitoring urban composition using ETM+ imagery. *Remote Sensing of Environment*, 93(4): 480–492. doi: 10.1016/j.rse.2004.08.003

Wu C S, Murray A T, 2003. Estimating impervious surface distribution by spectral mixture analysis. *Remote Sensing of Environment*, 84: 493–505. doi: 10.1016/S0034-4257(02)00136-0

Wu C S, Murray A T, 2005. A cokriging method for estimating population density in urban areas. *Remote Sensing for Urban Analysis*, 29: 558–579. doi: 10.1016/j.compenvurbsys.2005.01.006

Xiao R B, Ouyang Z Y, Zheng H *et al*., 2007. Spatial pattern of impervious surfaces and their impacts on land surface temperature in Beijing, China. *Journal of Environmental Sciences*, 19(2): 250–256. doi: 10.1016/S1001-0742(07)60041-2

Xie Miaomiao, Wang Yanglin, Fu Meichen *et al*., 2013. Pattern dynamics of thermal-environment effect during urbanization: a case study in Shenzhen City, China. *Chinese Geographical Science*, 23(1): 101–112. doi: 10.1007/s11769-012-0580-7

Xie Miaomiao, Wang Yanglin, Li Guicai *et al*., 2009. Thermal environment effect dynamic of landscape changes in different urbanization phases: a case study of western Shenzhen. *Geographical Research*, 28(4): 1085–1094. (in Chinese)

Yuan Chao, Wu Bingfang, Luo Xingshun *et al*., 2009. Estimating urban impervious surface distribution with RS. *Engineering of Surveying and Mapping*, 18(3): 32–39. (in Chinese)

Yue Wenze, 2009. Improvement of urban impervious surface estimation in Shanghai using Landsat7 ETM+ data. *Chinese Geographical Science*, 19(3): 283–290. doi: 10.1007/s11769-009-0283-x

Zhang M H, Qin Z H, Liu X *et al.*, 2003. Detection of stress in tomatoes induced by late blight disease in California, USA, using hyperspectral remote sensing. *International Journal of Applied Earth Observation and Geoinformation*, 4: 295–310. doi: 10.1016/S0303-2434(03)00008-4

Zhou Cunlin, Xu Hanqiu, 2007. A spectral mixture analysis and mapping of impervious surfaces in built-up land of Fuzhou City. *Journal of Image and Graphics*, 5: 875–881. (in Chinese)

Zhou Jianhua, Zhou Yifan, GuoXiaohua *et al*., 2011. Methods of extracting distribution information of plants at urban. *Journal of East China Normal University* (*Natural Science*), 6: 1–9. (in Chinese)